

Direct Detection of Dimethylstannylene and Tetramethyldistannene in Solution and the Gas Phase by Laser Flash Photolysis of 1,1-Dimethylstannacyclopent-3-enes

Rosa Becerra,[†] Peter P. Gaspar,^{*‡} Cameron R. Harrington,[§] William J. Leigh,^{*§} Ignacio Vargas-Baca,[§] Robin Walsh,^{*#} and Dong Zhou[†]

Contribution from the Instituto de Química-Física 'Rocasolano', C.S.I.C., C/Serrano 119, 28006 Madrid, Spain, Department of Chemistry, Washington University, St. Louis, Missouri 63130, Department of Chemistry, McMaster University, 1280 Main Street West, Hamilton, ON L8S 4M1 Canada, and School of Chemistry, University of Reading, Whiteknights, Reading, RG6 6AD U.K

Received April 25, 2005; E-mail: gaspar@wuchem.wustl.edu; leigh@mcmaster.ca; r.walsh@reading.ac.uk

Abstract: The photochemistry of 1,1-dimethyl- and 1,1,3,4-tetramethylstannacyclopent-3-ene (**4a** and **4b**, respectively) has been studied in the gas phase and in hexane solution by steady-state and 193-nm laser flash photolysis methods. Photolysis of the two compounds results in the formation of 1,3-butadiene (from **4a**) and 2,3-dimethyl-1,3-butadiene (from **4b**) as the major products, suggesting that cycloreversion to yield dimethylstannylene (SnMe₂) is the main photodecomposition pathway of these molecules. Indeed, the stannylene has been trapped as the Sn–H insertion product upon photolysis of **4a** in hexane containing trimethylstannane. Flash photolysis of **4a** in the gas phase affords a transient absorbing in the 450–520-nm range that is assigned to SnMe₂ by comparison of its spectrum and reactivity to those previously reported from other precursors. Flash photolysis of **4b** in hexane solution affords results consistent with the initial formation of SnMe₂ ($\lambda_{\max} \approx 500$ nm), which decays over ~ 10 μ s to form tetramethyldistannene (**5b**; $\lambda_{\max} \approx 470$ nm). The distannene decays over the next ca. 50 μ s to form at least two other longer-lived species, which are assigned to higher SnMe₂ oligomers. Time-dependent DFT calculations support the spectral assignments for SnMe₂ and Sn₂Me₄, and calculations examining the variation in bond dissociation energy with substituent (H, Me, and Ph) in disilenes, digermenes, and distannenes rule out the possibility that dimerization of SnMe₂ proceeds reversibly. Addition of methanol leads to reversible reaction with SnMe₂ to form a transient absorbing at $\lambda_{\max} \approx 360$ nm, which is assigned to the Lewis acid–base complex between SnMe₂ and the alcohol.

Introduction

There has been considerable interest over the past 3 decades in the chemistry of dialkyl and diaryl Sn(II) compounds ("stannylenes").^{1–5} Several stable derivatives have been reported,^{3,4} but remarkably little is known about the chemistry of simpler derivatives that are transient species at room temperature. Dimethylstannylene (SnMe₂) has received the greatest attention; some aspects of its chemistry in solution have been reported,^{6–10} as have its infrared spectrum in a matrix at low temperatures and ab initio calculations of its geometry and

electronic structure.¹¹ It has been detected directly in the gas phase only relatively recently, allowing study of its reactivity toward various reagents such as alkenes, dienes, alkynes, alcohols, alkyl halides, silicon and germanium hydrides, HCl, and SO₂.¹² To our knowledge, however, SnMe₂ has never been detected directly in solution by time-resolved spectroscopic methods.

For such studies to be successful, one needs a stable precursor that undergoes photodecomposition to yield the transient of interest cleanly and efficiently. The latter is crucial, because the lowest-energy absorption band in the electronic spectra of divalent group 14 compounds is characteristically weak, making these species particularly difficult to detect reliably when they are generated from precursors that are prone to other competing photoreactions or whose photolysis proceeds in low quantum yield. This has been demonstrated in some of our recent work on transient germlylenes in solution,^{13,14} and the same is expected

[†] Instituto de Química-Física 'Rocasolano'.

[‡] Washington University.

[§] McMaster University.

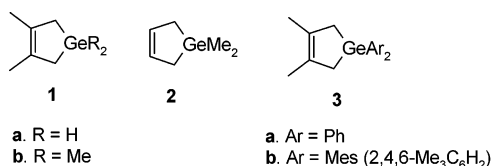
[#] University of Reading.

- (1) Neumann, W. P. *Chem. Rev.* **1991**, *91*, 311.
- (2) Driess, M.; Grutzmacher, H. *Angew. Chem., Int. Ed. Engl.* **1996**, *35*, 828.
- (3) Weidenbruch, M. *Eur. J. Inorg. Chem.* **1999**, 1999, 373.
- (4) Tokitoh, N.; Okazaki, R. *Coord. Chem. Rev.* **2000**, *210*, 251.
- (5) Boganov, S. E.; Egorov, M. P.; Faustov, V. I.; Nefedov, O. M. In *The Chemistry of Organic Germanium, Tin and Lead Compounds*; Rappoport, Z., Ed.; John Wiley and Sons: New York, 2002; Vol. 2, pp 749–839.
- (6) Neumann, W. P.; Schwarz, A. *Angew. Chem., Int. Ed. Engl.* **1975**, *14*, 812.
- (7) Grugel, C.; Neumann, W. P.; Seifert, P. *Tetrahedron Lett.* **1977**, *25*, 2205.
- (8) Gross, L. W.; Moser, R.; Neumann, W. P.; Scherping, K. H. *Tetrahedron Lett.* **1982**, *23*, 635.
- (9) Scherping, K. H.; Neumann, W. P. *Organometallics* **1982**, *1*, 1017.
- (10) Watta, B.; Neumann, W. P.; Sauer, J. *Organometallics* **1985**, *4*, 1954.

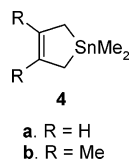
- (11) Bleckmann, P.; Maly, H.; Minkwitz, R.; Neumann, W. P.; Watta, B.; Olbrich, G. *Tetrahedron Lett.* **1982**, *23*, 4655.
- (12) Becerra, R.; Boganov, S. E.; Egorov, M. P.; Faustov, V. I.; Krylova, I. V.; Nefedov, O. M.; Walsh, R. *J. Am. Chem. Soc.* **2002**, *124*, 7555.
- (13) (a) Leigh, W. J.; Harrington, C. R.; Vargas-Baca, I. *J. Am. Chem. Soc.* **2004**, *126*, 16105. (b) Leigh, W. J.; Harrington, C. R. *J. Am. Chem. Soc.* **2005**, *127*, 5084.

to be true of other group 14 carbene analogues such as silylenes and stannylenes.

One of our groups has published several studies of the chemistry of GeH₂ in the gas phase, generated by 193-nm photolysis of 3,4-dimethylgermacyclopent-3-ene (**1a**),^{15–21} as well as two studies of GeMe₂, similarly obtained by photolysis of 1,1-dimethylgermacyclopent-3-ene (**2**).^{16,22} Following this and other even earlier leads,²³ others of us have recently shown that compounds of this general type are also very useful as precursors to substituted germynes such as dimethyl-, diphenyl-, and dimethylgermylene (GeMe₂, GePh₂, and GeMes₂, respectively) for study by time-resolved methods in solution.¹³ In each case, both the germylene and its (subsequently formed) digermene dimer can be detected and characterized by laser flash photolysis methods, using the substituted 1-germacyclopent-3-ene derivatives **1b** and **3a,b** in conjunction with either 193- or 248-nm excitation, depending on the absorption characteristics of the particular compound. A similar methodology has proven successful for the photochemical generation of reactive silylenes in solution.^{24,25}

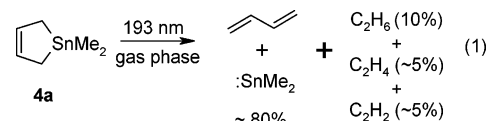


In this paper, we report the results of a study of the photochemistry of the potential SnMe₂ precursors **4a** and **4b** in the gas phase and in hexane solution by steady-state and laser flash photolysis methods. In the gas phase, **4a** affords a transient species with absorption characteristics similar to those previously obtained for SnMe₂ from other precursors,¹² and which exhibits similar reactivity toward stannylyne scavengers. Photolysis of **4b** in solution, where a much wider range of monitoring wavelengths are accessible, reveals a much richer transient behavior and provides kinetic details of the initial steps in the oligomerization of SnMe₂, which is known from earlier work to be the main fate of the species under such conditions.^{9,10}

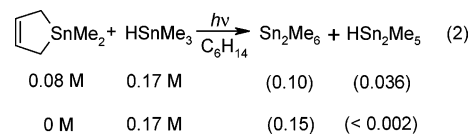


Results

Photochemical Product Studies. Gas chromatographic analysis of the volatile products from preparative 193-nm photolysis of **4a** in the gas phase (0.2 Torr **4a**, 100 Torr N₂ as buffer gas) indicates them to consist of 1,3-butadiene (ca. 80%), ethane (ca. 10%), ethylene (ca. 5%), and acetylene (ca. 5%) (eq 1). This is consistent with the extrusion of SnMe₂ as the major excited-state reaction pathway.



Photolysis of a deoxygenated 0.08 M solution of **4a** in hexane containing 0.17 M trimethylstannane (Me₃SnH) was carried out with 254-nm light; a similar solution containing only Me₃SnH (0.17 M) was photolyzed in parallel for comparison. GC/MS analysis of the photolyzates after ca. 10% conversion of **4a** allowed the detection of hexamethyldistannane (Sn₂Me₆) and a compound tentatively identified as pentamethyldistannane (HSn₂Me₅) on the basis of mass spectral evidence (see Supporting Information) as the only volatile tin-containing products; the latter was formed in roughly 30% of the yield of Sn₂Me₆ in the photolysis of the **4a**/HSnMe₃ mixture, but in only trace amounts in the photolysis of HSnMe₃ alone. The results, which are summarized in eq 2 as the product GC peak areas relative to internal standard in the two experiments, suggest that the Sn₂Me₆ formed is derived mainly from photolysis of HSnMe₃, whereas HSn₂Me₅ (the expected product of reaction of SnMe₂ with HSnMe₃) is derived from photolysis of **4a**.



Photolysis with a Zn resonance lamp (214 nm) of a deoxygenated 0.02 M solution of **4b** in cyclohexane-*d*₁₂ containing 0.5 M methanol (MeOH), with periodic monitoring of the photolyzate by (600 MHz) ¹H NMR spectroscopy, resulted in the formation of 2,3-dimethyl-1,3-butadiene (DMB) and a colorless precipitate that deposited on the walls of the NMR tube. A collection of very weak peaks was also present in the 0.5–0.8 ppm range of the spectrum (including a singlet at δ 0.53 ppm), consistent with (SnMe₂)_n oligomers,¹⁰ but no new signals were detectable in the δ 3.5–5.5 ppm region, where those due to Sn–H and Sn–OMe protons would be expected.²⁶ The conversion was ca. 12% after 2.5 h of photolysis and produced an 80–90% yield of DMB relative to consumed starting material. Virtually indistinguishable results were obtained upon photolysis for the same period of time of **4b** in cyclohexane-*d*₁₂ containing no added alcohol. It should be noted that the yields of DMB produced in the two experiments were identical within experimental error, indicating that the presence of the alcohol in concentrations as high as 0.5 M has no effect on the efficiency of the primary photoreaction of **4b**.

- (14) Harrington, C. R.; Leigh, W. J.; Chan, B. K.; Gaspar, P. P.; Zhou, D. *Can. J. Chem.* **2005**, *83*, 1324.
 (15) Becerra, R.; Walsh, R. *Phys. Chem. Chem. Phys.* **1999**, *1*, 5301.
 (16) Becerra, R.; Egorov, M. P.; Krylova, I. V.; Nefedov, O. M.; Walsh, R. *Chem. Phys. Lett.* **2002**, *351*, 47.
 (17) Becerra, R.; Bogdanov, S. E.; Egorov, M. P.; Faustov, V. I.; Promyslov, V. M.; Nefedov, O. M.; Walsh, R. *Phys. Chem. Chem. Phys.* **2002**, *4*, 5079.
 (18) Becerra, R.; Bogdanov, S. E.; Egorov, M. P.; Nefedov, O. M.; Walsh, R. *Chem. Phys. Lett.* **1996**, *260*, 433.
 (19) Becerra, R.; Bogdanov, S. E.; Egorov, M. P.; Faustov, V. I.; Nefedov, O. M.; Walsh, R. *Phys. Chem. Chem. Phys.* **2001**, *3*, 184.
 (20) Becerra, R.; Bogdanov, S. E.; Egorov, M. P.; Faustov, V. I.; Nefedov, O. M.; Walsh, R. *J. Am. Chem. Soc.* **1998**, *120*, 12657.
 (21) Becerra, R.; Walsh, R. *Phys. Chem. Chem. Phys.* **2002**, *4*, 6001.
 (22) Becerra, R.; Bogdanov, S. E.; Egorov, M. P.; Lee, V. Ya.; Nefedov, O. M.; Walsh, R. *Chem. Phys. Lett.* **1996**, *250*, 111.
 (23) Bobbitt, K. L.; Lei, D.; Maloney, V. M.; Parker, B. S.; Raible, J. M.; Gaspar, P. P. In *Frontiers of Organogermanium, -Tin and -Lead Chemistry*; Lukevics, E., Ignatovich, L., Eds.; Latvian Institute of Organic Synthesis: Riga, Latvia, 1993; pp 41–53.
 (24) Steinmetz, M. G.; Yu, C. *Organometallics* **1992**, *11*, 2686.

- (25) Jiang, P.; Gaspar, P. P. *J. Am. Chem. Soc.* **2001**, *123*, 8622.
 (26) Schumann, H.; Schumann, I. In *Gmelin Handbook of Inorganic Chemistry*; Krücker, U., Ed.; Springer-Verlag: Berlin, 1989; Part 17 (Sn; Organotin Compounds), pp 78–79.

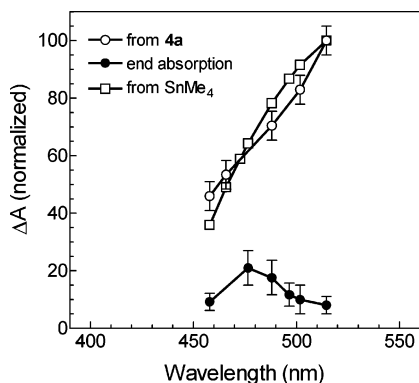


Figure 1. Transient absorption spectra obtained from 193-nm laser flash photolysis of **4a** (○, ●) and SnMe_4 (□) in the gas phase. The open symbols are the transient absorbance (ΔA) values obtained at the peak of the excitation pulse. The solid points and curve represent the residual ΔA values at the end of the time window monitored (50–100 μs).

Laser Flash Photolysis of **4a** in the Gas Phase at 193 nm.

For investigation of the transient spectrum, sample mixtures were made up containing ca. 30 mTorr of **4a** in 10 Torr of SF_6 . Laser (193-nm) photolysis gives a transient species with strong absorptions in the accessible monitoring range of 457.9–514.5 nm. The spectrum in this range has its strongest absorption at 514.5 nm and matches those obtained previously from other precursors to SnMe_2 (e.g., SnMe_4).¹² The absorptions decay to final steady, nonbaseline values. The intensities of these end absorptions vary with wavelength, apparently peaking at ca. 480 nm. Whether the end absorptions are due to a stable final product (i.e., stable for hours) or a much more slowly decaying transient cannot be determined from these results, but the ratio of end absorption to initial absorption ($I_{\text{final}}/I_{\text{initial}}$) appears to be independent of the initial transient concentration over a range of a factor of 4. Figure 1 shows a comparison of transient spectra obtained from 193-nm flash photolysis of **4a** and SnMe_4 ,¹² normalized at 514.5 nm (100%).

At $\lambda = 501.7$ nm, transient decays were studied using precursor pressures between 11 and 44 mTorr (in SF_6 , 10 Torr). The decays fit acceptably to first-order kinetics over a minimum of 70% consumption of the transient with essentially no variation of the decay constant [$(5.5 \pm 1.5) \times 10^4 \text{ s}^{-1}$] with precursor pressure over this range. Even at the highest precursor pressure, there was no evidence of a second-order component to the decay.

Kinetic studies were undertaken with a variety of substrates (MeOH, HCl, SO_2 , and 2-butyne) using both 501.7 and 514.5 nm as monitoring wavelengths, which were chosen to minimize the effects of end absorption. However, all of the substrates seem to quench the initial photochemical yield of the transient (SnMe_2) partially. This enhances the distorting effect of end absorption, making kinetic analysis more difficult, and also has the effect of limiting the maximum values obtainable for decay constants. This might be because, at high substrate pressures, the decay trace is complicated by formation of the other absorbing species (viz, the end absorption), which affects the kinetics. An example of data obtained with SO_2 as the substrate is shown in Figure 2, along with the corresponding data obtained previously using SnMe_4 as the precursor.¹² As can be seen, the data points obtained here are in reasonable agreement with those obtained previously, although at higher partial pressures of SO_2 , they diminish slightly from the earlier values. This was also true for reactions with HCl and MeOH. The effect was not

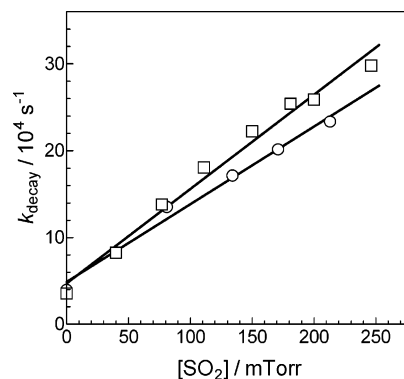


Figure 2. Plots of k_{decay} vs SO_2 pressure, from 193-nm laser flash photolysis of **4a** (○) and SnMe_4 (□)¹² in the gas phase.

Table 1. Absolute Rate Constants for Reaction of the Transient Produced upon 193-nm Laser Flash Photolysis of **4a** in the Gas Phase at 298 K^a

substrate	$k/10^9 \text{ M}^{-1} \text{ s}^{-1}$	
	this work	ref 12
SO_2	17.1 ± 0.9	20.2 ± 0.8
HCl	0.40 ± 0.04	0.49 ± 0.020
MeOH	1.25 ± 0.07	1.57 ± 0.04
2-butyne	2.32 ± 0.12	4.72 ± 0.07

^a Rate constants converted from molecular units.

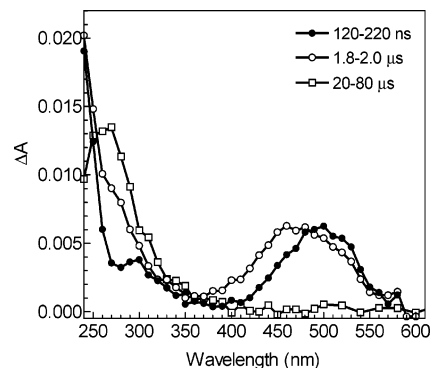


Figure 3. Transient absorption spectra, recorded by 193-nm flash photolysis of **4b** in deoxygenated hexane solution at 25 °C, 0.12–0.220 (●), 1.8–2.0 (○), and 20–80 (□) μs after the laser pulse.

observed with 2-butyne, but the reaction seemed to be significantly slower than observed previously. The absolute values for the rate constants obtained from these experiments, using only the lower decay constant values, are collected in Table 1.

Laser Flash Photolysis of **4b in Solution.** Solution-phase laser flash photolysis experiments with **4b** were carried out with the pulses from an ArF excimer laser (193 nm, ca. 25 ns, ca. 50 mJ), using rapidly flowing (ca. 5 mL min^{-1}) deoxygenated solutions of **4b** (ca. 3×10^{-5} M) in dry hexane. Transient absorptions were monitored over the 240–650-nm wavelength range through several time windows after the laser pulse. At least three different transient species were observed to form and decay over a time scale of ca. 40 ms, which was the longest time scale monitored in our experiments. Figure 3 shows transient absorption spectra recorded 120–220 ns, 1.8–2.0 μs , and 20–80 μs after excitation, and Figure 4 shows representative transient decay/growth profiles recorded at monitoring wavelengths of 530, 450, and 260 nm. As the two figures show, laser photolysis causes the prompt formation of a species absorbing with an apparent λ_{max} of ~ 500 nm, the bulk of which decays

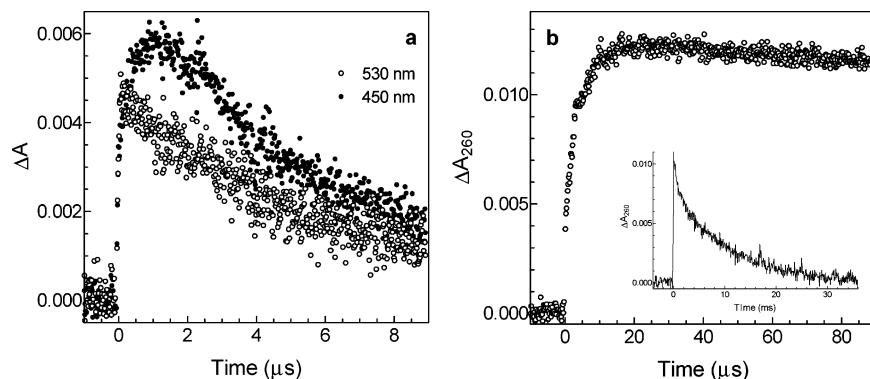


Figure 4. Transient decay/growth profiles, recorded by 193-nm flash photolysis of **4b** in deoxygenated hexane solution at 25 °C at monitoring wavelengths of (a) 530 and 450 nm and (b) 260 nm. The inset in (b) shows a trace recorded at 260 nm over a full scale of 40 ms.

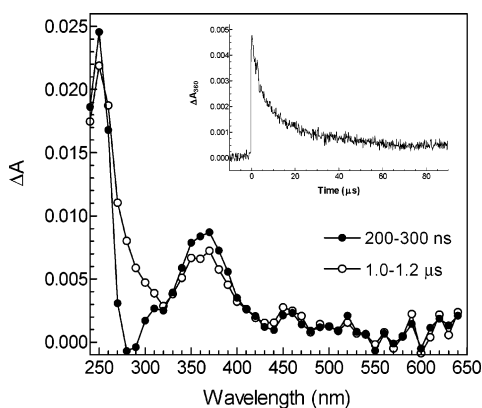
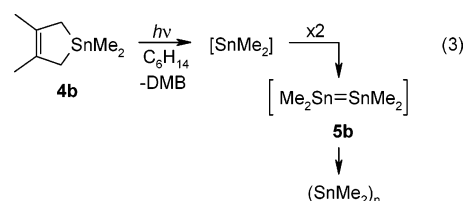


Figure 5. Transient absorption spectra, recorded by 193-nm flash photolysis of a ca. 3×10^{-5} M solution of **4b** in dry deoxygenated hexane containing 3 mM MeOH at 23 °C, recorded 0.2–0.3 and 1.0–1.2 μ s after the laser pulse. The weak absorption band centered at ca. 460 nm is real and is due to Sn_2Me_4 (**5b**). The inset shows a typical transient decay trace, recorded at a monitoring wavelength of 360 nm.

over ca. 10 μ s. A decay trace recorded at 540 nm over a factor of 10 longer time scale fits well to second-order kinetics (see Supporting Information), yielding a second-order decay constant of $k/\epsilon_{540} = (1.4 \pm 0.1) \times 10^7 \text{ cm s}^{-1}$, where ϵ_{540} is the molar extinction coefficient at 540 nm. A second transient species ($\lambda_{\text{max}} \approx 470 \text{ nm}$) is observed to be formed after the laser pulse, reaching a maximum in concentration ca. 1 μ s after the pulse and then decaying with complex kinetics over the next 20–30 μ s (see Figure 4 and Supporting Information). All of this is accompanied by the slower growth of a stronger transient signal centered at 260 nm, which decays with complex kinetics and an apparent lifetime of ca. 10 ms. The growth of these absorptions occurs over a time scale similar to that of the decay of the longer-wavelength transients, suggesting that they are produced by reaction of the latter species. Furthermore, the complexity of their temporal behavior suggests that they are due to more than one long-lived species.

We assign the first-formed transient to SnMe_2 ($\lambda_{\text{max}} \approx 500 \text{ nm}$); the second-formed transient to its dimerization product, tetramethyldistannene (**5b**; $\lambda_{\text{max}} \approx 470 \text{ nm}$); and the more slowly formed species observed in the 240–300-nm range to one or more SnMe_2 oligomers, formed by reaction of **5b** (eq 3). Several comments regarding the time evolution of the transient signals due to these species are warranted. First, there is substantial spectral overlap between the 500- and 470-nm species, which makes quantitative interpretation of the transient decays very difficult. Indeed, decays recorded even at the long- and short-

wavelength edges of the two absorption bands over longer time scales show strong similarities to one another, which might be interpreted as the result of equilibrium between the two species. Second, the fact that the apparent growth of the (470-nm) signal assigned to **5b** is much more rapid than the decay of the signal assigned to SnMe_2 does *not* represent an inconsistency in its assignment; the growth of the second-formed transient appears to be much more rapid than it actually is because the onset of the decay of this species occurs quite early after it is initially formed. Finally, the lifetime measured for the 260-nm transient absorptions ($\tau \approx 10 \text{ ms}$) should be considered a very crude lower limit, as the longest lifetime our system is capable of measuring accurately in the configuration used for these experiments is ca. 3 ms.

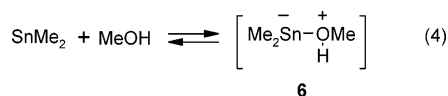


Addition of MeOH (0.2–3.0 mM) to the solution resulted in significant reductions in the intensities of the signals due to SnMe_2 and **5b**, but had little effect on the decay or growth times of either species. In the case of the SnMe_2 absorption (monitored at 530 nm), a ca. 4-fold drop in intensity was observed at the highest concentration of alcohol employed; at none of the concentrations examined could a fast initial decay of the signal be resolved. Similarly, the absorptions due to **5b** (monitored at 440 nm) suffered a ca. 3-fold drop in maximum intensity over the 0.2–3.0 mM concentration range, but there was no change in the growth time of the signal and only small changes in the decay time. These reductions in signal strength are much larger than can be explained by screening of the excitation light by the alcohol, which has a molar extinction coefficient of $\epsilon_{193} = 39 \pm 1 \text{ dm}^3 \text{ mol}^{-1} \text{ cm}^{-1}$ at 193 nm in hydrocarbon solvents.²⁷ Single-exponential decay analysis of a transient decay profile recorded at 440 nm in the presence of 3 mM MeOH afforded a reasonable fit and yielded a pseudo-first-order decay rate constant of $k_{\text{decay}} = (8.4 \pm 0.7) \times 10^4 \text{ s}^{-1}$. The signal at 260 nm developed a fast growth component whose contribution increased at the expense of the slow component with increasing methanol concentration, until at 3 mM MeOH, the latter was

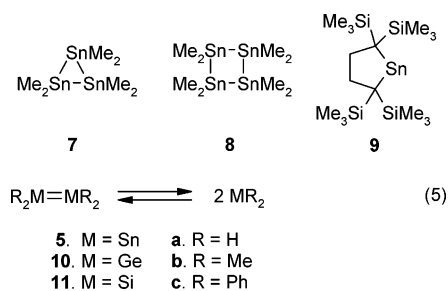
(27) Kerst, C.; Byloos, M.; Leigh, W. J. *Can. J. Chem.* **1997**, *75*, 975.

no longer apparent in the transient profile; although the overall decay rate appeared to increase slightly, there were only small reductions in the maximum strength of the absorption over the 0.2–3.0 mM range in MeOH concentration.

These changes were accompanied by the appearance of a new transient absorption centered at 360 nm, which appeared to be formed within the duration of the laser pulse at the lowest MeOH concentration employed (0.2 mM). The maximum absorbance of the species increased with increasing MeOH concentration, and the signal decayed with clean second-order kinetics and a decay constant of $k/\epsilon_{360} = (7.2 \pm 0.3) \times 10^6 \text{ cm}^{-1} \text{ s}^{-1}$, which did not vary significantly with MeOH concentration over the 1–3 mM range. Figure 5 shows a transient absorption spectrum recorded 1–1.2 μs after the pulse in the presence of 3 mM MeOH, along with a transient decay trace recorded at 360 nm. We assign the transient to the Lewis acid–base complex of SnMe₂ and MeOH (**6**; eq 4).



DFT Calculations. Time-dependent density functional theory (TD-DFT) calculations were carried out to predict the electronic spectra of SnMe₂, tetramethyldistannene (**5b**), and the three- and four-membered cyclic SnMe₂ oligomers **7** and **8**, as well as that of the stable stannylene **9** in order to assess the reliability of the method employed through comparison to the known X-ray crystal structure and UV absorption spectrum of the compound.²⁸ Spectral calculations for SiMe₂ and Si₂Me₄ (**11b**) were also carried out at the same level of theory, to allow comparisons with experimental spectra for the complete series of dimethylmetallylenes and tetramethyldimetallenes. To address the question of possible reversibility in the dimerization of SnMe₂ (vide supra), we also calculated bond dissociation energies for the series of distannenes, digermenes, and disilenes **5a–c**, **10a–c**, and **11a–c**, respectively (eq 5). Frequency calculations were carried out on the H- and methyl-substituted derivatives, to obtain the zero-point energy corrections, internal energies, and entropies.



Geometry optimizations employed the exchange and correlation functionals of Perdew and Wang (PW91)²⁹ and uncontracted Slater-type orbitals of triple- ζ double-polarization (TZ2P) quality as basis functions, as we used previously for calculation of the structures and electronic spectra of the corresponding germlylenes (GeH₂, GeMe₂, and GePh₂), the germanium analogue of stannylene **9**, and digermenes **10a–c**.^{13a} Relativistic effects

were included in the calculations for the Sn-containing species. Electronic spectral calculations were then carried out on the optimized geometries of SnMe₂, **5b**, **7–9**, SiMe₂, and **11b** using the SAOP exchange-correlation potential,^{30,31} with the same triple- ζ double-polarization basis sets and relativistic adjustments as were employed for the geometry optimizations; the latter were used in the calculations of the spectra of the silicon-containing species as well. We previously showed this method to afford excitation energies for **10a–c** and the corresponding germlylenes that agree with experimental values to within 0.12 eV or less.^{13a} The relevant computed structural parameters for each of the molecules studied are listed in the Supporting Information.

Comparison of the calculated structure of **9** to the reported X-ray structure of the compound²⁸ (see Supporting Information) revealed reasonable agreement between experiment and theory, although not quite as good as we found earlier for the homologous germlylene derivative.^{13a} The calculated Sn–C distance and C–Sn–C angle in **9** are 2.25 Å and 85.7°, respectively, which should be compared to 2.22 Å and 86.7° in the experimental structure.²⁸ The calculated structures of the other MR₂ and the M₂R₄ species (M = Si, Ge, Sn; R = H, Me, Ph) show the expected changes with increasing atomic number of the group 14 elements [i.e., increasing M–R distances and decreasing R–M–R angles in both species, as well as increasing M–M bond distances and pyramidalization angles in the (trans-bent) dimetallenes]. The structures of the parent and methylated compounds generally compare quite favorably with the results of previous DFT calculations for the MH₂,³² M₂H₄,^{33–38} MMe₂,^{39,40} and M₂Me₄^{37,38} species. They also agree reasonably well with ab initio results, particularly for the Ge- and Sn-containing species.^{41–52}

Geometry optimizations for the dimetallenes were carried out under C_i symmetry in all cases; however, **5b** was also optimized without symmetry constraints after rotating the Sn=Sn bond in the C_i-symmetric (trans-bent) structure to a non-zero value. This afforded a nonsymmetric trans-bent structure with a twist angle of 11.78° about the Sn=Sn bond, but with otherwise almost identical structural features to the C_i-symmetric conformer. The

- (30) Gritsenko, O. V.; Schipper, P. R. T.; Baerends, E. J. *Chem. Phys. Lett.* **1999**, *302*, 199.
- (31) Schipper, P. R. T.; Gritsenko, O. V.; van Gisbergen, S. J. A.; Baerends, E. J. *J. Chem. Phys.* **2004**, *112*, 1344.
- (32) Su, M.-D. *J. Phys. Chem. A* **2002**, *106*, 9563.
- (33) Jacobsen, H.; Ziegler, T. *J. Am. Chem. Soc.* **1994**, *116*, 3667.
- (34) Kapp, J.; Remko, M.; Schleyer, P. v. R. *Inorg. Chem.* **1997**, *36*, 4241.
- (35) Chen, W.-C.; Su, M.-D.; Chu, S.-Y. *Organometallics* **2001**, *20*, 564.
- (36) Mosey, N. J.; Baines, K. M.; Woo, T. K. *J. Am. Chem. Soc.* **2002**, *124*, 13306.
- (37) Malcolm, N. O. J.; Gillespie, R. J.; Popelier, P. L. A. *J. Chem. Soc., Dalton Trans.* **2002**, 3333.
- (38) Su, M.-D. *J. Phys. Chem. A* **2004**, *108*, 823.
- (39) Su, M.-D.; Chu, S.-Y. *J. Phys. Chem. A* **1999**, *103*, 11011.
- (40) Su, M.-D. *Chem. Eur. J.* **2004**, *10*, 6073.
- (41) Fjeldberg, T.; Haaland, A.; Schilling, B. E. R.; Lappert, M. F.; Thorne, A. *J. Chem. Soc., Dalton Trans.* **1986**, 1551.
- (42) Goldberg, D. E.; Hitchcock, P. B.; Lappert, M. F.; Thomas, K. M.; Thorne, A. J.; Fjeldberg, T.; Haaland, A.; Schilling, B. E. R. *J. Chem. Soc., Dalton Trans.* **1986**, 2387.
- (43) Liang, C.; Allen, L. C. *J. Am. Chem. Soc.* **1990**, *112*, 1039.
- (44) Grev, R. S.; Schaefer, H. F., III; Baines, K. M. *J. Am. Chem. Soc.* **1990**, *112*, 9458.
- (45) Trinquier, G. *J. Am. Chem. Soc.* **1990**, *112*, 2130.
- (46) Windus, T. L.; Gordon, M. S. *J. Am. Chem. Soc.* **1992**, *114*, 9559.
- (47) Karni, M.; Apeloig, Y. *J. Am. Chem. Soc.* **1990**, *112*, 8589.
- (48) Boatz, J. A.; Gordon, M. S.; Sita, L. R. *J. Phys. Chem.* **1990**, *94*, 5488.
- (49) Heaven, M. W.; Metha, G. F.; Buntine, M. A. *J. Phys. Chem. A* **2001**, *105*, 1185.
- (50) Hajgato, B.; Takahashi, M.; Kira, M.; Veszpremi, T. *Chem. Eur. J.* **2002**, *8*, 2126.
- (51) Szabados, A.; Hargittai, M. *J. Phys. Chem. A* **2003**, *107*, 4314.
- (52) Becerra, R.; Cannady, J. P.; Walsh, R. J. *J. Phys. Chem. A* **2004**, *108*, 3987.

(28) Kira, M.; Yauchibara, R.; Hirano, R.; Kabuto, C.; Sakurai, H. *J. Am. Chem. Soc.* **1991**, *113*, 7785.

(29) Perdew, J. P.; Chevary, J. A.; Vosko, S. H.; Jackson, K. A.; Pederson, M. R.; Singh, D. J.; Fiolhais, C. *Phys. Rev. B* **1992**, *46*, 6671.

Table 2. Calculated and Experimental UV–Vis Absorption Maxima for Stannylene **9**; SnMe₂; and SnMe₂ Oligomers **5b**, **7**, and **8**^a

compound	λ_{\max} (nm) [E (eV)]	
	calcd	exptl
9	505 [2.46], 346 [3.58], 281 [4.49], 271 [4.57]	484 [2.56], 370 [3.35], 285 [4.35], 247 [5.02] ^b
SnMe ₂	502 [2.47], 239 [5.17]	500 [2.50]
Me ₂ Sn=SnMe ₂ (5b)	C _i : 445 [2.79] unsym: 447 [2.78]	470 [2.64]
cyclo-(SnMe ₂) ₃ (7)	298 [4.16]	
cyclo-(SnMe ₂) ₄ (8)	308 (sh) [4.02], 249 [4.97], 239 [5.19]	

^a sh = shoulder. ^b Reference 28.

total bonding energies in the two structures differed by only 0.2 kcal mol⁻¹, in keeping with a rather flat potential energy surface for twisting about the Sn=Sn bond.³³ Electronic spectral calculations were also carried out for this conformer and revealed no significant differences in either the position or the intensity of the longest-wavelength absorption band compared to those for the C₇-symmetric structure. The calculated Sn–Sn bond distance in **5b** matches almost precisely the experimental value ($r_{\text{Sn–Sn}} = 2.768 \text{ \AA}$) reported for the stable tetraalkyldistannane Sn₂(CH(SiMe₃)₂)₄.⁴²

The calculated Sn–Sn bond distances in **7** and **8** are within the ranges reported experimentally for those stable cyclotristannanes^{53,54} and cyclotetrastannanes^{55–58} that have been characterized crystallographically, and are close to the values calculated for the parent compounds by ab initio methods.⁵⁹ The calculated structure of **8** is puckered with a fold angle of 39.6°, a larger deviation from planarity than those in reported experimental structures, in which the fold angles range from 0° to ca. 30° depending on substituent.^{55–58} Previous ab initio calculations on cyclotetrastannane (cyclo-Sn₄H₈) predicted the molecule to be planar.⁵⁹

The results of the electronic spectral calculations for the stannylenes and (SnMe₂)_n oligomers are summarized in Table 2 along with the corresponding experimental values of Kira and co-workers for **9**²⁸ and those of the present work for SnMe₂ and Sn₂Me₄ (**5b**). There is excellent agreement between the predicted and experimental spectra of the stannylenes in both cases, as well as with previous calculations of the absorption maximum of SnMe₂ using ab initio and TD-DFT methods.¹² Similarly, the predicted values of the lowest-energy absorption bands in the UV–vis spectra of SiMe₂ [$\lambda_{\max} = 457 \text{ nm}$ (2.71 eV)] and tetramethyldisilene [**11b**; $\lambda_{\max} = 365 \text{ nm}$ (3.39 eV)] (see Supporting Information) fall within or just outside the ranges in experimental values ($\lambda_{\max} = 453\text{--}470 \text{ nm}$ ^{60–64} and

Table 3. Calculated Total Bonding Energy, Enthalpy, and Free Energy Changes for Dissociation of Dimetallenes R₂M=MR₂ to the Corresponding Metallylenes^a

M	R = H	R = Me	R = Ph
ΔE (kcal mol ⁻¹) ^b			
Si	70.4	60.2	51.1
Ge	53.4	43.7	35.0
Sn	33.9	29.0	24.1
ΔH° (kcal mol ⁻¹) ^c			
Si	66.3	56.0	—
Ge	49.6	39.9	—
Sn	30.9	25.8	—
ΔS° (cal mol ⁻¹ K ⁻¹) ^c			
Si	34.6	39.2	—
Ge	34.9	37.6	—
Sn	31.5	32.6	—
ΔG° (kcal mol ⁻¹) ^c			
Si	56.0	44.3	—
Ge	39.2	28.7	—
Sn	21.5	16.1	—

^a Values for M = Sn include relativistic corrections. ^b At 0 K; not corrected for zero-point energy contributions. ^c Corrected for zero-point energy contributions.

344–360 nm,^{65,66} respectively). In the case of **9**, although the calculated oscillator strength for the first transition [Sn(*n*,p); $f = 0.004$] is comparable to the experimental value of 0.006, the intensity of the second band is significantly overestimated. This transition corresponds to promotion of a Si–C(σ) bonding electron to the Sn(p) LUMO. This same discrepancy was evident in our calculations of the spectra of the germanium analogue of this molecule^{13a} and was essentially independent of the size of the basis set and the potential model used for the calculation of excitations.

Table 3 summarizes the results of the bond dissociation energy (BDE) calculations for the three series of hydrido-, methyl-, and phenyl-substituted dimetallenes, in the form of total energies (at 0 K) for all nine compounds and zpe-corrected standard enthalpies and free energies for the hydrido- and methyl-substituted derivatives (at 298 K). The entropy changes required for calculation of the latter quantities are also included in the table. The smallest values of ΔS° were obtained for the distannenes, consistent with the weaker M=M bonds and lower energies for the rocking modes that disappear upon dissociation, compared to the disilenes and digermenes. To help assess the accuracy of the calculation for **5b**, we also calculated the Sn–Sn BDE in hexamethyldistannane. The value obtained, $\Delta E = 68.8 \text{ kcal mol}^{-1}$, corresponds to $\Delta H^\circ \approx 66 \text{ kcal mol}^{-1}$, assuming reasonable values for the internal energy and zpe corrections. This can be compared to the best current experimental estimate of $\Delta H^\circ = 68.5 \pm 2.0 \text{ kcal mol}^{-1}$.⁶⁷

Discussion

Most aspects of the photochemistry of **4a** and **4b**, including the transient spectroscopic behavior, bear strong qualitative similarities to those observed previously for the germacyclo-

- (53) Cardin, C. J.; Cardin, D. J.; Constantine, S. P.; Drew, M. G. B.; Rashid, H.; Convery, M. A.; Fenske, D. *J. Chem. Soc., Dalton Trans.* **1998**, 2749.
 (54) Masamune, S.; Sita, L. R.; Williams, D. J. *J. Am. Chem. Soc.* **1983**, *105*, 630.
 (55) Lappert, M. F.; Leung, W. P.; Raston, C. L.; Thorne, A. J.; Skelton, B. W.; White, A. H. *J. Organomet. Chem.* **1982**, *233*, C28.
 (56) Puff, H.; Bach, C.; Reuter, H.; Schuh, W. *J. Organomet. Chem.* **1984**, *277*, 17.
 (57) Puff, H.; Bach, C.; Schuh, W.; Zimmer, R. *J. Organomet. Chem.* **1986**, *312*, 313.
 (58) Cardin, C. J.; Cardin, D. J.; Convery, M. A.; Devereux, M. M.; Kelly, N. B. *J. Organomet. Chem.* **1991**, *414*, C9.
 (59) Rubio, J.; Illas, F. *J. Mol. Struct. (THEOCHEM)* **1984**, *110*, 131.
 (60) Michalczyk, M. J.; Fink, M. J.; De Young, D. J.; Carlson, C. W.; Welsh, K. M.; West, R.; Michl, J. *Silicon, Germanium, Tin Lead Compds.* **1986**, *9*, 75.
 (61) Baggott, J. E.; Blitz, M. A.; Frey, H. M.; Lightfoot, P. D.; Walsh, R. *Int. J. Chem. Kinet.* **1992**, *24*, 127.

- (62) Baggott, J. E.; Blitz, M. A.; Frey, H. M.; Walsh, R. *J. Am. Chem. Soc.* **1990**, *112*, 8337.
 (63) Baggott, J. E.; Blitz, M. A.; Frey, H. M.; Lightfoot, P. D.; Walsh, R. *J. Chem. Soc., Faraday Trans. 2* **1988**, *84*, 515.
 (64) Levin, G.; Das, P. K.; Bilgrien, C.; Lee, C. L. *Organometallics* **1989**, *8*, 1206.
 (65) Yamaji, M.; Hamanishi, K.; Takahashi, T.; Shizuka, H. *J. Photochem. Photobiol. A: Chem.* **1994**, *81*, 1.
 (66) Sekiguchi, A.; Maruki, I.; Ebata, K.; Kabuto, C.; Sakurai, H. *J. Chem. Soc., Chem. Commun.* **1991**, 341.

pentene derivatives **1**–**3**^{13a,15–23} and are consistent with formal cheletropic cycloreversion to yield SnMe₂ and the corresponding conjugated diene as the primary photochemical reaction of these molecules. In the gas phase, flash photolysis of **4a** affords a transient product with UV–vis spectrum and reactivity similar to those assigned previously to SnMe₂ in experiments with other photochemical precursors to the molecule.¹² Likewise, laser photolysis of **4b** in solution leads to behavior that is strikingly similar to that observed from the related germanium compounds **1a** and **3a,b**, which was attributed to the initial formation of the corresponding germylene derivatives (GeMe₂, GePh₂, and GeMe₂, respectively) followed by the products of dimerization (the corresponding digermenes) and then their subsequent oligomerization products.^{13a} In all four cases (viz, **1a**, **3a,b**, and **4b**), this process is characterized by the sequential formation of species that absorb at successively shorter wavelengths than the initially formed transient and exhibit successively longer lifetimes, as would be expected. We thus assign the initially formed species from laser photolysis of **4b** to SnMe₂ ($\lambda_{\max} \approx 500$ nm); the second one to its dimerization product, tetramethyldistannene (**5b**; $\lambda_{\max} \approx 470$ nm); and the long-lived species absorbing below 300 nm to higher SnMe₂ oligomers (eq 3).

The absorption spectrum of the stannylene in solution is similar to that measured in the gas-phase experiments, although because of instrumental limitations, we have been able to detect only the short-wavelength rising edge of the gas-phase absorption band. Qualitative comparisons of the (1–2 μ s) time scale over which the initial decay of the stannylene and the growth of its primary product occur to that observed in previous experiments with GePh₂ (for which a rate constant for dimerization of $k_{\text{dim}} = 1.1 \times 10^{10} \text{ M}^{-1} \text{ s}^{-1}$ has been measured^{13a}) suggest that the dimerization of SnMe₂ in solution proceeds at a similar rate. This is consistent with the second-order decay constant measured at 540 nm of $k/\epsilon_{540} = (1.4 \pm 0.1) \times 10^7 \text{ cm s}^{-1}$; if we assume that the extinction coefficient of the stannylene at its absorption maximum is on the order of $1000 \text{ dm}^3 \text{ mol}^{-1} \text{ cm}^{-1}$ (cf. that for SiMe₂^{68,69}), a value of $k \approx 7 \times 10^9 \text{ M}^{-1} \text{ s}^{-1}$ is obtained for the absolute rate constant for dimerization. To our knowledge, the product of this reaction, tetramethyldistannene (**5b**), has not been detected directly before under any set of conditions.

Comparison of the experimental spectra of SnMe₂ ($\lambda_{\max} = 500$ nm), GeMe₂ ($\lambda_{\max} = 480$ nm),^{22,70} and SiMe₂ ($\lambda_{\max} = 453$ – 465 nm)^{60,64} reveals a consistent trend toward decreasing excitation energy with increasing size of the group 14 element, similar to that exhibited by **9** ($\lambda_{\max} = 484 \text{ nm}^{28}$) and its Ge and Si analogues ($\lambda_{\max} = 450 \text{ nm}^{71}$ and 440 nm^{72} respectively). The trend is reproduced reasonably faithfully by the TD-DFT calculations, which predict lowest-energy absorption maxima of 502, 463, and 457 nm for SnMe₂, GeMe₂,^{13a} and SiMe₂, respectively. Calculations using the same method for the

corresponding dimetallenes (**5b**, **10b**, **11b**) predict a similar trend in absorption maxima for these compounds, with predicted values of $\lambda_{\max} = 445$, 374, and 365 nm for the distannene, digermene, and disilene, respectively. The agreement between the predicted and experimental solution-phase spectra of Ge₂Me₄ (**10b**; $\lambda_{\max} = 370 \text{ nm}$)^{13a,73,74} and Si₂Me₄ (**11b**; $\lambda_{\max} = 360 \text{ nm}$)⁶⁵ is again outstanding and affords a considerable degree of confidence in the ability of the theoretical method to predict the position of the lowest-energy absorption band in Sn₂Me₄ (**5b**) with reasonable accuracy. We can thus be fairly certain that the spectrum that grows in over the first ca. 1 μ s after pulsed laser photolysis of **4b** is due to the distannene ($\lambda_{\max} \approx 470$ nm), shifted to the blue of the stannylene absorption band but overlapped partially with it.

Interestingly, the temporal behaviors of the transient signals observed at the long- and short-wavelength edges (e.g., 530–540 and 430–450 nm, respectively) of the broad transient absorptions observed upon flash photolysis of **4b** in solution differ considerably from one another only in the first ca. 2 μ s after the laser pulse and then follow qualitatively similar time dependences thereafter. These similarities presumably result simply from the substantial overlap in the spectra of the two species. Nevertheless, we considered in some detail the alternative possibility, that this behavior results from reversible interconversion of the stannylene and distannene over the time scale of their eventual removal from the system via oligomerization.

The possibility seems a reasonable one, as most of the stable acyclic distannenes that are currently known are dissociative in solution.^{42,75–80} These compounds all contain sterically bulky substituents, and most are tetraaryl-substituted; the individual effects of steric and electronic factors on the Sn=Sn bond strengths in these compounds are not clear.⁸¹ We thus decided to expand the scope of our DFT calculations on SnMe₂ and **5b** to examine the predicted variations in bond dissociation energy of the Sn=Sn bond as a function of substituent, by bracketing the value for the tetramethyl system with those for the parent distannene (for which previous calculations have been reported^{33,34,44}) and tetraphenyldistannene (**5c**), as a model for the known tetraaryldistannenes that are dissociative in solution. To provide a benchmark for the calculations on the tin systems, we also carried out similar calculations for the corresponding digermenes (**10**) and disilenes (**11**) (Table 3) and hexamethyldistannane, all using the same theoretical method.

The trend of decreasing BDE with increasing atomic number of the group 14 element, which is observed in the present

- (67) Martinho Simoes, J. A.; Liebman, J. F.; Slayden, S. W. In *The Chemistry of Organic, Germanium, Tin and Lead Compounds*; Patai, S., Ed.; John Wiley & Sons Ltd.: New York, 1995; Vol. 1, pp 245–266.
- (68) Drahnak, T. J.; Michl, J.; West, R. *J. Am. Chem. Soc.* **1979**, *101*, 5427.
- (69) Raabe, G.; Vancik, H.; West, R.; Michl, J. *J. Am. Chem. Soc.* **1986**, *108*, 671.
- (70) Mochida, K.; Tokura, S. *Bull. Chem. Soc. Jpn.* **1992**, *65*, 1642.
- (71) Kira, M.; Ishida, S.; Iwamoto, T.; Ichinohe, M.; Kabuto, C.; Ignatovich, L.; Sakurai, H. *Chem. Lett.* **1999**, *1999*, 263.
- (72) Kira, M.; Ishida, S.; Iwamoto, T.; Kabuto, C. *J. Am. Chem. Soc.* **1999**, *121*, 9722.

- (73) Mochida, K.; Kayamori, T.; Wakasa, M.; Hayashi, H.; Egorov, M. P. *Organometallics* **2000**, *19*, 3379.
- (74) Taraban, M. B.; Volkova, O. S.; Plyusnin, V. F.; Ivanov, Y. V.; Leshina, T. V.; Egorov, M. P.; Nefedov, O. M.; Kayamori, T.; Mochida, K. *J. Organomet. Chem.* **2000**, *601*, 324.
- (75) Goldberg, D. E.; Harris, D. H.; Lappert, M. F.; Thomas, K. M. *J. Chem. Soc., Chem. Commun.* **1976**, 261.
- (76) Klinkhammer, K. W.; Schwarz, W. *Angew. Chem., Int. Ed. Engl.* **1995**, *34*, 1334.
- (77) Weidenbruch, M.; Kilian, H.; Peters, K.; von Schnering, H. G.; Marsmann, H. *Chem. Ber.* **1995**, *128*, 983.
- (78) Klinkhammer, K. W.; Fassler, T. F.; Grutzmacher, H. *Angew. Chem., Int. Ed.* **1998**, *37*, 124.
- (79) Della Bona, M. A.; Cassani, M. C.; Keates, J. M.; Lawless, G. A.; Lappert, M. F.; Sturmman, M.; Weidenbruch, M. *J. Chem. Soc., Dalton Trans.* **1998**, 1187.
- (80) Sturmman, M.; Saak, W.; Klinkhammer, K. W.; Weidenbruch, M. *Z. Anorg. Allg. Chem.* **1999**, *625*, 1955.
- (81) (a) Power, P. P. *J. Chem. Soc., Dalton Trans.* **1998**, 2939. (b) Power, P. P. *Chem. Rev.* **1999**, *99*, 3463.

calculations for all three substituents, is well established from earlier *ab initio* and DFT calculations for the parent dimetalloenes.^{33,34,44} Our calculated ΔE values (0 K, *zpe*-corrected) for disilene (**11a**; 65.6 kcal mol⁻¹), digermene (**10a**; 49.1 kcal mol⁻¹), and distannene (**5a**; 30.7 kcal mol⁻¹) are all higher than values calculated previously with other methods,^{33,34,44} but the present value for **11a** comes closest to the experimental value of 63.3 kcal mol⁻¹, reported by Ruscic and Berkowitz.⁸² The agreement with experimental data is also excellent in the case of the BDE of hexamethyldistannane (*vide supra*).

The calculations for the methyl- and phenyl-substituted systems reveal a successive reduction in BDE throughout the three series of dimetalloenes as the hydrogens in the parent compounds are replaced with methyl and phenyl substituents. This can be interpreted in terms of a substituent effect on the stabilities of the corresponding metallylenes. What is known of the differences in the reactivities of the parent metallylenes compared to those of the dimethyl analogues for the silicon and germanium analogues supports this view; both SiMe₂^{61–63,83} and GeMe₂^{16,22} are substantially less reactive than the corresponding parent molecules in the gas phase.^{84–86} Recent results for GePh₂ in solution indicate that it exhibits similar or slightly lower reactivity than GeMe₂ in all cases that have been studied so far, although the comparisons that have been made were necessarily confined to gas-phase rate constants for the simpler germylene, because of a lack of reliable solution-phase values for reactions with the same or similar substrates.^{13b}

Table 3 also contains the calculated values of ΔG° for dissociation of the parent dimetalloenes and tetramethyldimetalloenes. The value of $\Delta G^\circ = 16.1$ kcal mol⁻¹ for **5b** is roughly 10 kcal mol⁻¹ higher than the value required by the experimental data if dimerization of SnMe₂ is reversible. The latter was estimated assuming a concentration of ca. 10 μ M for the amount of SnMe₂ produced by the laser pulse (which is consistent with the typical transient absorbances observed in our solution-phase experiments and an extinction coefficient of ca. 1000 dm³ mol⁻¹ cm⁻¹), with the assumption that roughly half of it remains after the conversion to **5b** comes to equilibrium. This leads to an estimate of $K_{\text{eq}} \approx 10^{-5}$ M for the equilibrium constant for dissociation of the distannene and a value of $\Delta G^\circ \approx 5$ kcal mol⁻¹, assuming that dimerization was fully reversible under the conditions of our experiments. The comparison ignores solvation effects, but such effects can be expected to be small considering that, in hexane solution, the only solvation interaction possible is that due to dispersion forces. Despite the uncertainties in these estimates, the calculations would appear to rule out reversibility.

The zero-point energy contributions to the dissociation energies are in the ranges of 3.2–4.8 kcal mol⁻¹ for the parent dimetalloenes and 2.5–4.1 kcal mol⁻¹ for the tetramethyl derivatives, with the largest values being obtained for the disilenes and the smallest for the distannenes. Applying similar corrections to the calculated ΔE values for the phenylated systems affords estimates of ca. 48, 32, and 21 kcal mol⁻¹ for the BDEs of **11c**, **10c**, and **5c**, respectively, at 298 K. This then

leads to estimates of ca. 36, 20, and 11 kcal mol⁻¹ for the expected ΔG° values for dissociation of the three derivatives, assuming reasonable values for the entropy changes. The estimated ΔG° for **5c** can be compared to the 0–2 kcal mol⁻¹ value that would be required for the reported “dissociative” tetraaryldistannenes.⁷⁵ The reason these distannenes are dissociative, while **5b** is not, must be ascribed to steric factors, which appear to contribute as much as 8–10 kcal mol⁻¹ to the dissociation energies of these highly hindered derivatives.

The question naturally arises from the solution studies as to whether distannene **5b** might also be formed in detectable amounts in the gas phase. We believe that it is, based on the rather close match between the gas-phase end absorptions and the spectrum assigned to **5b** in solution (Figure 1), as well as the kinetic arguments presented in the following discussion. Similar long-lived absorptions, as well as the formation of solid precipitates (so-called “dust”), were evident in the experiments with the four other SnMe₂ precursors that were studied previously.¹²

The gas-phase decays of SnMe₂ were quite noisy, but they fit reasonably well to single exponentials and showed no obvious second-order kinetic component; the decay constants (k_{dec}) varied over the range $(4\text{--}7) \times 10^4$ s⁻¹, but did not vary systematically with variations in the initial transient concentration over a factor of 4, as would be expected if dimerization contributed significantly to the decay kinetics. We thus conclude that a pseudo-first-order decay process is mainly responsible for the decay of the stannylene in the gas-phase experiments. This process can most likely be identified as surface reactions with the solid particulates that cannot be removed by pumping the reaction vessel, as the lack of dependence of the decay rate constants on precursor pressure in the absence of added scavengers rules out pseudo-first-order reaction with the precursor (**4a**).

Nevertheless, the kinetic analyses can accommodate a contribution of 5–15% from dimerization, which corresponds roughly to the yield of **5b** that is indicated by the relative intensities of the initial and end absorptions in our experiments, given that the calculations (see Supporting Information) predict the extinction coefficient of **5b** to be ca. 10 times greater than that of SnMe₂ at the respective absorption maxima. Similar differences are predicted for germylens and their digermene dimers and have been corroborated experimentally in the case of the GeMe₂/Ge₂Me₄ system.^{13a} The rate constant required to give this amount of dimer is estimated to be $k_{\text{rec}} \approx 8 \times 10^9$ M⁻¹ s⁻¹ (see Supporting Information), which is in good agreement with the solution value ($\sim 7 \times 10^9$ M⁻¹ s⁻¹) obtained in this work and is about a factor of 20 less than the collision rate. We have also verified by RRKM calculations that SnMe₂ recombination in the gas phase should not be significantly pressure-dependent under our experimental conditions (see Supporting Information). We note, however, that the end absorptions were also present in decays obtained in the presence of stannylene scavengers, although we did not examine them near their absorption maxima.

Turning briefly to the products formed in solution over the longer time scale, it is clear from the form of the growth/decay profiles that their formation is linked to the decay of SnMe₂ and **5b**, and so they can be assigned to higher SnMe₂ oligomers with some degree of confidence. The decay kinetics of the

(82) Ruscic, B.; Berkowitz, J. J. *Chem. Phys.* **1991**, *95*, 2416.

(83) Baggott, J. E.; Blitz, M. A.; Frey, H. M.; Lightfoot, P. D.; Walsh, R. *Chem. Phys. Lett.* **1987**, *135*, 39.

(84) Jasinski, J. M.; Becerra, R.; Walsh, R. *Chem. Rev.* **1995**, *95*, 1203.

(85) Becerra, R.; Walsh, R. *Res. Chem. Kinet.* **1995**, *3*, 263.

(86) Bogdanov, S. E.; Egorov, M. P.; Faustov, V. I.; Krylova, I. V.; Nefedov, O. M.; Becerra, R.; Walsh, R. *Russ. Chem. Bull., Int. Ed.* **2005**, *54*, 483.

signals recorded in the 240–300-nm monitoring range are complex, and we tentatively interpret them as consisting of at least two components, at least one of which exhibits a lifetime in excess of 10 ms. The calculated UV absorption spectra of the three- and four-membered cyclic oligomers of SnMe₂ (**7** and **8**, respectively) indicate that these two compounds could well contribute to the transient absorptions observed in this spectral range. Unfortunately, it is not possible to be any more specific than that in regard to the identities of these species; the observed absorption maximum ($\lambda_{\text{max}} = 265 \text{ nm}$, $E = 4.68 \text{ eV}$) is closest to that calculated for cyclotetrastannane **8**, but the level of agreement is rather poor. No UV spectral data for compounds of these types have been reported, to our knowledge.

The remaining set of data to be discussed is that obtained from flash photolysis of **4b** in hexane containing methanol, one of the few reactive scavengers that can be studied in solution with 193-nm laser excitation.^{27,87–89} The gas-phase results indicate that SnMe₂ reacts with MeOH with a rate constant of ca. $1.2 \times 10^9 \text{ M}^{-1} \text{ s}^{-1}$ (see Table 1 and ref 12). Interestingly, we were unable to detect any acceleration of the decay of SnMe₂ in solution in the presence of the alcohol; the only effects noted were a marked reduction in the intensities of the signals due to the stannylene and distannene over the 0.2–3 mM range in alcohol concentration, with the effect on the stannylene signal being the greater. Furthermore, there was no change in the growth time of the distannene signal over this concentration range either. Despite this, the product of the reaction can be readily detected in the form of a new, long-lived transient absorbing with $\lambda_{\text{max}} \approx 360 \text{ nm}$, which decays with second-order kinetics (Figure 3) and is assigned to the Lewis acid–base complex of the stannylene with the alcohol (**6**; eq 3). The recent theoretical calculations of Su predict this species to be the primary product in the reaction of SnMe₂ with MeOH, and predict an activation energy of at least 15 kcal mol⁻¹ for its further reaction to yield the formal O–H insertion product, methoxydimethylstannane.⁴⁰ The magnitude of this barrier could explain why the methoxystannane is in fact *not* formed in detectable amounts in steady-state trapping experiments (vide supra); the ultimate fate of SnMe₂ in the latter experiments, even in the presence of relatively high concentrations of alcohol, is oligomerization. Few examples of stable alkoxydialkylhydridostannanes are known,^{26,90,91} but water and MeOH are known to undergo oxidative addition to Lappert's stannylene {Sn[CH(SiMe₃)₂]₂} to afford the corresponding (stable) O–H insertion products.⁹¹ The reaction was proposed to proceed via initial formation of the corresponding stannylene–alcohol (water) complex, but if this complex can rearrange readily to product, then the required H migration must either have a lower barrier than that calculated by Su for the SnMe₂–MeOH complex (**6**)⁴⁰ or proceed catalytically.

Because screening of the excitation light and excited-state quenching effects can both be discounted as possible trivial reasons for the drop in the signal strengths upon addition of the alcohol, the only reasonable remaining explanation that is

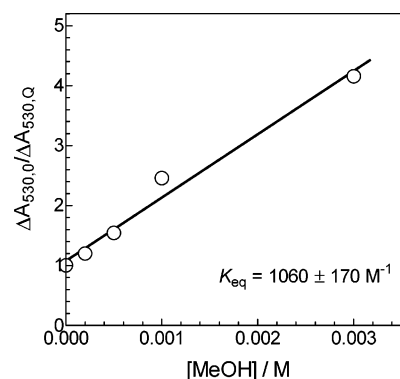


Figure 6. Plot of the ratio of initial transient absorbances due to SnMe₂ (monitored at 530 nm) in the absence and presence of MeOH ($\Delta A_{530,0}$ and $\Delta A_{530,Q}$, respectively) vs [MeOH]. The solid line represents the least-squares fit of the data to eq 6.

consistent with the effects noted above is fast, *reversible* reaction of SnMe₂ with the alcohol to yield complex **6**. We thus interpret the stannylene transient absorptions measured in the presence of MeOH as being due to residual free stannylene present in rapid equilibrium with the complex. Under such conditions, the signal intensities due to residual free stannylene are related to the equilibrium constant for the reaction according to eq 6, where ΔA_0 and ΔA_Q are the initial transient absorbances in the absence and presence of the alcohol at concentration [Q], respectively; K_{eq} is the equilibrium constant for reaction; and the excitation laser intensity is roughly constant throughout the experiment. A plot of the data according to eq 6 is shown in Figure 6; the slope is the equilibrium constant, $K_{\text{eq}} = 1060 \pm 170 \text{ M}^{-1}$. This corresponds to a free energy difference of ca. 2 kcal mol⁻¹ in favor of the complex in hexane solution at 298 K, in reasonable agreement with the recent calculations of Su,⁴⁰ with appropriate assumptions as to entropic factors. It should be noted that, with an equilibrium constant on the order of 1000 M⁻¹, the forward rate constant for the process would need to be less than ca. $5 \times 10^9 \text{ M}^{-1} \text{ s}^{-1}$ in order for us to be able to distinguish an initial fast decay (due to the approach to equilibrium) from noise under the conditions of our experiments. This limit is defined mainly by the strength of the transient signals obtained, which was rather low in the present study, but is somewhat higher than the absolute rate constant ($k \approx 10^9 \text{ M}^{-1} \text{ s}^{-1}$) determined earlier for reaction of SnMe₂ with MeOH in the gas phase. As the latter was determined at relatively low pressures and pressure dependence has not been studied, it might well be significantly lower than the value in solution.

$$\Delta A_0 / \Delta A_Q = 1 + K_{\text{eq}}[Q] \quad (6)$$

The SnMe₂–MeOH complex decays with clean second-order kinetics and a rate coefficient of $k/\epsilon_{360} = (7.2 \pm 0.3) \times 10^6 \text{ cm} \text{ s}^{-1}$ in the presence of 3 mM alcohol, similar to the value determined from the decay of the stannylene in the absence of added MeOH. The extinction coefficients of the complex (Figure 5) and the free stannylene (Figure 3) at their respective absorption maxima appear to be quite similar to one another, so it can be concluded that the presence of the alcohol at low concentrations has little effect on the overall dimerization rate. In the limit where dimerization proceeds only by combination of free SnMe₂ molecules, the overall rate constant is expected to be reduced from its value in the absence of the alcohol by

(87) Kerst, C.; Boukherroub, R.; Leigh, W. J. *J. Photochem. Photobiol. A: Chem.* **1997**, *110*, 243.

(88) Leigh, W. J.; Boukherroub, R.; Kerst, C. *J. Am. Chem. Soc.* **1998**, *120*, 9504.

(89) Leigh, W. J.; Kerst, C.; Boukherroub, R.; Morkin, T. L.; Jenkins, S.; Sung, K.; Tidwell, T. T. *J. Am. Chem. Soc.* **1999**, *121*, 4744.

(90) Hayashi, K.; Iyoda, J.; Shihara, I. *J. Organomet. Chem.* **1967**, *10*, 81.

(91) Schager, F.; Goddard, R.; Seevogel, K.; Porschke, K. R. *Organometallics* **1998**, *17*, 1546.

the factor $K_{\text{eq}}[\text{MeOH}]$, or a factor of roughly 3 in the presence of 3 mM MeOH. The observed reductions in the strength of the signal due to **5b** in the presence of the alcohol are consistent with the idea that formation of the distannene does not involve dimerization of the complex, but proceeds via reaction of free stannylene in solution, either with itself or with the complex with which it is in equilibrium.

In contrast to the substantial reactivity exhibited by SnMe_2 with MeOH, our results indicate that tetramethyldistannene (**5b**) is relatively unreactive toward the alcohol; from the pseudo-first-order decay rate constant measured in the presence of 3 mM MeOH, an upper limit of ca. $3 \times 10^7 \text{ M}^{-1} \text{ s}^{-1}$ can be estimated for the absolute rate constant for the reaction.

Summary and Conclusions

Strong evidence has been obtained for the formation of highly reactive dimethylstannylene (SnMe_2) from the 193-nm photolysis of rational stannacyclopentene precursors (**4a**) in the gas phase and (**4b**) in solution. Steady-state photolysis in both cases leads to formation of the corresponding dienes, and in solution, SnMe_2 has been trapped by reaction with Me_3SnH to afford a product that has been tentatively identified as $\text{Me}_3\text{SnSnMe}_2\text{H}$, the product of Sn–H insertion.

Laser flash photolysis of **4b** in solution produces a sequence of transient species with partially overlapping broad-band spectra, led by formation of strong absorptions at 500 nm, followed by 470 nm, and eventually 260 nm. These are assigned to SnMe_2 , Sn_2Me_4 , and higher SnMe_2 oligomers (possibly *cyclo*- Sn_3Me_6 or *cyclo*- Sn_4Me_8), respectively, on the basis of both their time evolutions and their calculated (TD-DFT) spectra. The dimerization of SnMe_2 is very rapid, proceeding at close to the diffusion-controlled rate.

The same long-wavelength (500 nm) transient absorption band is observed in the gas-phase experiments, coincident with earlier observations of SnMe_2 generated from other precursors. Long-lived absorptions are also observed in the 450–515-nm wavelength region in the gas-phase experiments, following the decay of the SnMe_2 signal. The kinetic and spectroscopic evidence indicates that these could very well be due to Sn_2Me_4 , formed in minor yield by dimerization of the primary intermediate. Gas-phase trapping kinetics are broadly consistent with earlier studies.

In solution, the spectral overlap of the bands from SnMe_2 and Sn_2Me_4 makes it difficult to determine whether SnMe_2 dimerizes irreversibly or reaches an equilibrium with Sn_2Me_4 , but the latter possibility can be ruled out on the basis of DFT calculations of the bond dissociation energy of the distannene. The calculations we have undertaken include comparisons of geometries and transition energies with both the analogous germanium and silicon systems, as well as those for the parent (hydrogenated) and phenyl-substituted counterparts. The limited experimental data available are in excellent agreement with these calculations, providing a high level of confidence in comparisons between analogous molecules based on elements in different rows of the periodic table.

Addition of MeOH in solution leads to the formation of a new transient species absorbing at 360 nm, which is assigned

to the Lewis acid–base complex $\text{Me}_2\text{SnO}(\text{H})\text{Me}$, in equilibrium with free SnMe_2 and MeOH. The equilibrium constant ($K_{\text{eq}} \approx 1000 \text{ M}^{-1}$) is too low to allow measurement of the rate constant for the association process, but the data allow a lower limit of $k > 5 \times 10^9 \text{ M}^{-1} \text{ s}^{-1}$ to be established. This is consistent with the value of $k \approx 1 \times 10^9 \text{ M}^{-1} \text{ s}^{-1}$ measured in the gas phase at low pressure. The complex appears to decay by redissociation followed by SnMe_2 dimerization.

Sn_2Me_4 has not previously been observed directly under any set of conditions. SnMe_2 has been detected previously only in the gas phase, although instrumental limitations prevented the absorption maximum of this species from being observed under those conditions. The successful determination of the complete UV–vis absorption spectra of these two species achieved in this work strengthens our understanding of organotin(II) chemistry. Further work on these and related heavy carbene and alkene systems is in progress in our laboratories.

Experimental Section

The solvent hexanes (EMD Omnisolv) was purified by repeated washing with concentrated sulfuric acid, followed by distilled water, and preliminary drying over anhydrous sodium sulfate. It was then refluxed for several days under nitrogen over sodium/potassium amalgam and distilled. Deoxygenated samples of the solvent exhibited an absorbance of ca. 0.2 at 193 nm in a 7×7 mm quartz cell. Methanol (Sigma-Aldrich) was distilled from Mg/I_2 . The 1-stannacyclopent-3-enes **4a** and **4b** were prepared as recently described,⁹² and **4a** was further purified before use by vacuum distillation. Spectroscopic data for these compounds are listed in the Supporting Information.

All gases used in this work were deoxygenated thoroughly prior to use. Commercial samples of reactive substrates used were obtained as follows: 2-Butyne (GC purity > 99%) was from Cambrian Gases. HCl (>99%) and MeOH (Gold label, >99%) were from Sigma-Aldrich. SO_2 (99.5%) was from BDH.

The instrumentation and procedures employed for gas- and solution-phase laser flash photolysis experiments and details of the computational methods employed are summarized in the Supporting Information.

Acknowledgment. We thank the following for financial support: the Natural Sciences and Engineering Research Council (NSERC) of Canada, the Canada Foundation for Innovation and the Ontario Innovation Trust (W.J.L., C.R.H., and I.V.-B.), the DGICYT (Spain) under Project BQU2002-03381 (R.B.), the Royal Society for a Spain–U.K. Joint Project grant (No. 15636; R.W.), and the United States National Science Foundation under Grants CHE-9981715 and CHE-0316124 (P.P.G. and D.Z.).

Supporting Information Available: Details of the experimental and computational procedures employed in this work, computed geometric parameters and excitation energies, RRKM calculations and kinetic derivations, spectroscopic data for **4a** and **4b**, transient decay profiles recorded in hexane over extended time scales, experimental data used for the estimation of the equilibrium constant for methanol complexation, and details of the steady-state trapping experiments. This material is available free of charge via the Internet at <http://pubs.acs.org>.

JA052675D

(92) Zhou, D. Ph.D. Thesis, Washington University, St. Louis, MO, 2004.